JOURNAL OF MATERIALS SCIENCE 37 (2002) 941 – 947

Pore morphology and pore surface roughening in rocks: a small-angle neutron scattering investigation

D. SEN, S. MAZUMDER
Solid State Physics Division, Bhabha Atomic Research Centre, Trombay, Mumbai 400 085, India
E-mail: debasis@apsara.barc.ernet.in

S. TARAFDAR
Condensed Matter Physics Research Centre, Physics Department, Jadavpur University, Calcutta 700032, India

Pore morphology and pore-matrix interface roughening in some metamorphosed sedimentary rocks, sandstones and igneous rocks have been investigated using small-angle neutron scattering (SANS), in the length scales of ~20–1000 nm., which reveal the fractal nature of the rock-pore interfaces. Surface fractal dimension of the metamorphosed rocks and the sandstones has been estimated to be ~2.8 while, that for the igneous rocks has been found to be ~2.3. An attempt has been made to explain the relatively high surface fractal nature of the former rocks with the help of a computer simulation model based on the formation mechanisms of these rocks. SANS data indicate some ideas about the upper cut-off of the fractal geometry for the igneous rocks as well as for the sandstone, but no unambiguous cut-off value has been obtained for the metamorphosed rocks in the accessible length scale. The multiple scattering effect in these rock specimens has also been looked into by performing the SANS experiments for the two thicknesses on each specimen.

1. Introduction

Microstructure of rocks is a subject of practical importance and scientific interest from the petrologic point of view. Rocks can be considered as nearly two-phase systems, as perceived by neutrons, consisting of solids and pores separated by random surfaces. The solid phase generally consists of the minerals like feldspars, quartz, gypsum, calcite etc. Degrees of continuity of solid phase of a rock mostly influence the strength of a rock while the transport properties are mostly controlled by the connectivity of the pores and the random interface of the solid and the pore.

There has been considerable interest in studying the geometry of the rock-pore interface recently [1–7] and most of the works, experimental [1–4] as well as computer simulations [5, 6], are devoted to the nature of the rock-pore interface and the growth of correlated pore-scale structures. Avnir *et al.* [8] first showed, using Brauner-Emmet-Teller (BET) molecular absorption method, that various rock specimens posses fractal geometry. The origin of the term 'fractal' is due to the fact that some objects or some processes show a self-similarity over a wide length scale and posses some fractional dimension. Many properties of the fractal systems can often be described by quantities those are proportional to a power of another quantity. This relation is frequently called a power law. Here it is interesting to note that most of the fractal objects encountered in nature are self-affine and are generally random i.e., they are not created by the deterministic rules like for the Sierpinski gasket [9]. It is noteworthy that self-similar fractals rescale the same way along any spatial direction but self-affine fractals require different rescaling factors.

In a rock formation process, qualitatively, a number of small events occur closely to one another in time and space with few large events occurring in the same temporal and spatial region which lead to physical mechanisms that favours the power law scaling in the system and in turn prefers the interface to fluctuate rather than to stay flat. These fluctuations increase the surface area relative to smooth surface. In thermodynamics language one can say that the surface tension becomes negative [3, 10]. As the environmental conditions and the other physical parameters like temperature, pressure and altitude affect the process of rock formation, the fractal geometry and the fractal dimension for rocks are non-universal although it has been seen that the value of the fractal dimension always lies between 2 and 3.

Depending on the type of rock formation mechanisms, rocks can be mainly classified as (a) sedimentary, (b) igneous and (c) metamorphic. Sedimentary rocks, as the name suggests, originate from accumulation of

small grains of sand or clay often together with organic materials. Sedimentation takes place through the action of wind and water and leads to a highly porous (50–80%) unconsolidated agglomerate. The sedimentation process is then followed by compaction and diagenesis causing the unconsolidated mass to become a consolidated rock by flow of a pore filling fluids accompanied by the dissolution and other chemical processes. While approaching secular equilibrium between the matrix and formation brine the interface evolves by maximizing the internal surface area in response to the different driving forces like cation substitution and dissolution. Formation of igneous rocks takes place by the cooling or the solidification of magma. The rate of cooling has an important effect on size of the grain and the pores. Chemical composition, pressure and dissolved vapours also affect the pore structure. Metamorphic rocks are those, which have been so changed sometimes by the action of heat or pressure of the magmatic fluids that they can no longer be referred readily to their proper class.

Most of the peninsulas of India are constituted by Precambrian rocks and are covered by Phanerozoic sedimentary suites and Deccan plateau basalts [11]. The sedimentary assemblages include rocks formed when India was still a part of Gondwanaland, during the Paleozoic and much of the Mesozoic. They are mostly thin sequences, except in rift valleys, and are absent from much of the interior India. The Deccan plateau basalts, formed during the late Cretaceous to Early Tertiary and have been widely regarded as a volcanic consequence of the rifting of India from other parts of Gondwanaland, cover a large part of western and central India.

Small angle scattering (SAS) technique is an important and non-destructive technique to investigate the pore morphology and the roughness on the matrix-void interface in porous materials [1–4, 12–14] over a length scale of 1–1000 nm. The technique can also distinguish between the types of fractal geometry, volume or surface fractal. It is noteworthy that with a conventional SAS instrument, one can achieve a resolution up-to a length scale of 100 nm. However, with a moderate or high-resolution instrument, based on double crystal geometry, it is possible to achieve a resolution up-to a length scale of 1000 nm. or even more [15].

In this paper, we present the moderate-resolution small-angle neutron scattering (SANS) investigations on various rock specimens collected from different parts of India from the viewpoint of nature and the quantitative analysis of fractal geometry of the rock-pore interface. An attempt has been made to explain the fractal nature in metamorphosed sedimentary rocks and sandstone with the help of a computer simulation model, based on the formation mechanism of the above rocks.

2. Experimental

Rock specimens from different parts of India have been collected for SANS investigations. Three specimens (Specimen 1–3), collected from Devoprayag in Himalayan region, are of metamorphosed sedimentary in nature, which possess some layered structure. From places near Mumbai, in Deccan trap basalt regions, three rocks specimens (Specimens 4–6), igneous in nature, have been collected. Another sandstone specimen (Sample 7) has been collected from Barakar, situated in the Singhbhum zone of India. As-received metamorphosed and sandstone rocks were cut out in bedding-plane to different thicknesses and used for SANS measurements. Unlike the metamorphosed and the sandstone, the igneous rocks specimens have been found to be very hard without any layered structure and could not be thinned infinitely.

SANS experiments have been performed using a double crystal based moderate resolution small-angle neutron scattering instrument at the Guide Tube Laboratory of Dhruva reactor at Trombay, India [15]. The instrument consists of a non-dispersive (1,−1) setting of 111 reflections from silicon single crystals with specimen between the two crystals. The scattered intensities have been recorded as a function of wave vector transfer q [$=4\pi \sin(\theta)/\lambda$, where 2θ is the scattering angle and λ ($=0.312$ nm.) is the incident neutron wavelength for the present experiment]. The specimens under SANS investigations were placed on a sample holder with a circular slit of 1.5 cm. diameter. In order to study the multiple scattering effects in the above specimens, SANS experiments have been performed for two different thicknesses of each specimen. The measured SANS profiles have been corrected for background and resolution effects [16]. Fig 1. shows the corrected SANS profiles for specimens 1–3, plotted in double logarithmic scale. Figs 2–4 demo the profiles for the specimens 4–6 respectively. The profiles of the specimen 7 are depicted in Fig 5. Scanning electron micrographs (SEM) (using JEOL-5200) of the specimen 7 are presented in Fig 6.

3. Data interpretation and discussion

SANS profile from a specimen maps the size and shape of the scattering length density inhomogeneities in a material. For an object with fractal geometry, this technique can be used to determine the fractal dimension and the nature of fractal morphology [17, 18]. Bale and Schmidt [17] have derived an expression for the correlation function $g(r)$ for a surface fractal object with surface fractal dimension d_s, an intensive property of matter that offers a quantitative measure of the degree of surface roughness. After introducing the concept of the upper cut-off (ξ), the maximum size up-to which a surface can be viewed as a fractal, $g(r)$ can be expressed as

$$g(r) = \exp\left(-\frac{r}{\xi}\right)\left[1 - \left(\frac{S_o}{4\phi(1-\phi)V}\right)\left(\frac{r}{\xi}\right)^{3-d_s}\right] \tag{1}$$

where ϕ represents the fraction of the solid phase in the sample volume V, S_o is a constant in the measurement of the total surface. Scattering function $I(q)$ can be obtained by the Fourier transform of Equation 1 and is

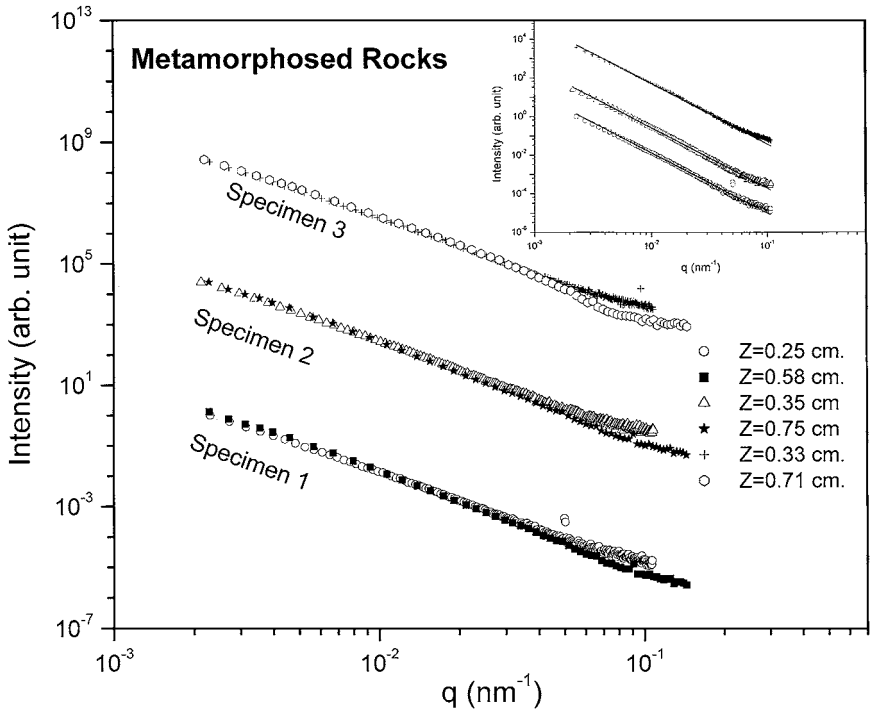

Figure 1 Corrected SANS profiles of specimens 1–3 (Sedimentary rocks from Deoprayaga) for two different thicknesses. The solid lines in the inset show the fit to the data from thinner specimens.

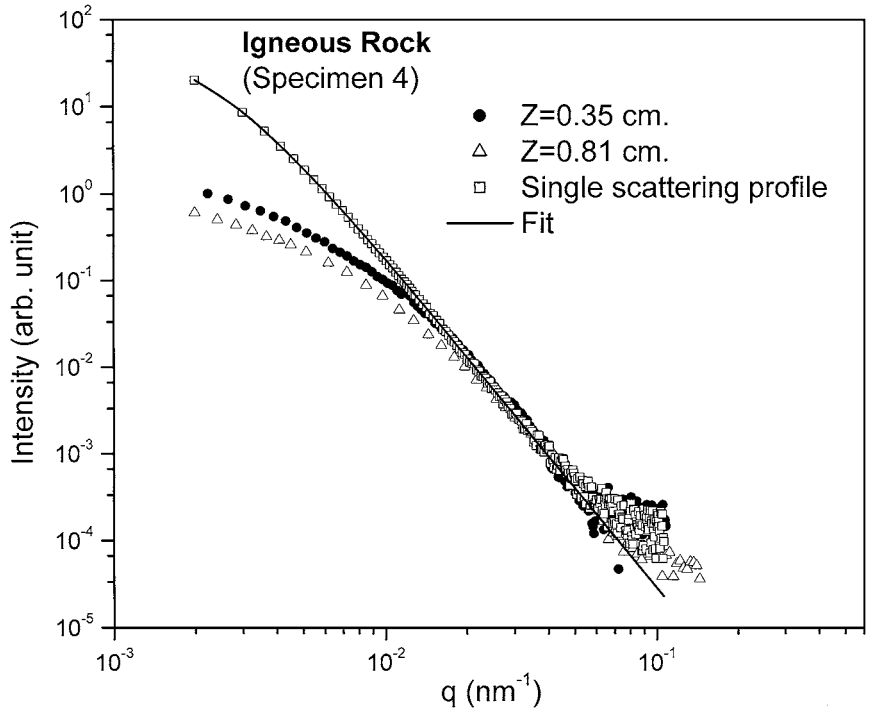

Figure 2 Corrected SANS profiles from specimen-4 (igneous rock) for two thicknesses. The estimated single scattering profile is also shown along-with the fit.

given by

$$I(q) = \text{const}\, q^{-1}\Gamma(5-d_s)\xi^{5-d_s}[1+(q\xi)^2]^{\frac{(d_s-5)}{2}} \times \sin[(d_s-1)\arctan(q\xi)] \quad (2)$$

For $\xi \gg 1/q$, the above equation reduces to a simplified power law relation

$$I(q) = \text{const}\, q^{d_s-6} \quad (3)$$

Equations 2 and 3 show that for a surface fractal object, the scattering profile should exhibit a power law behaviour over a wide q range and the exponent should be in a range -4.0 to -3.0 as the value of surface fractal dimension d_s may vary between 2.0 to 3.0. The closer the value of d_s to 2.0 implies a surface that is closer to smooth surface. The surface with perfect smooth boundary, i.e. $d_s = 2.0$, the Equation 3 turns into the conventional Porod law.

All the above expressions for $I(q)$ are based upon the single scattering approximation and are valid when

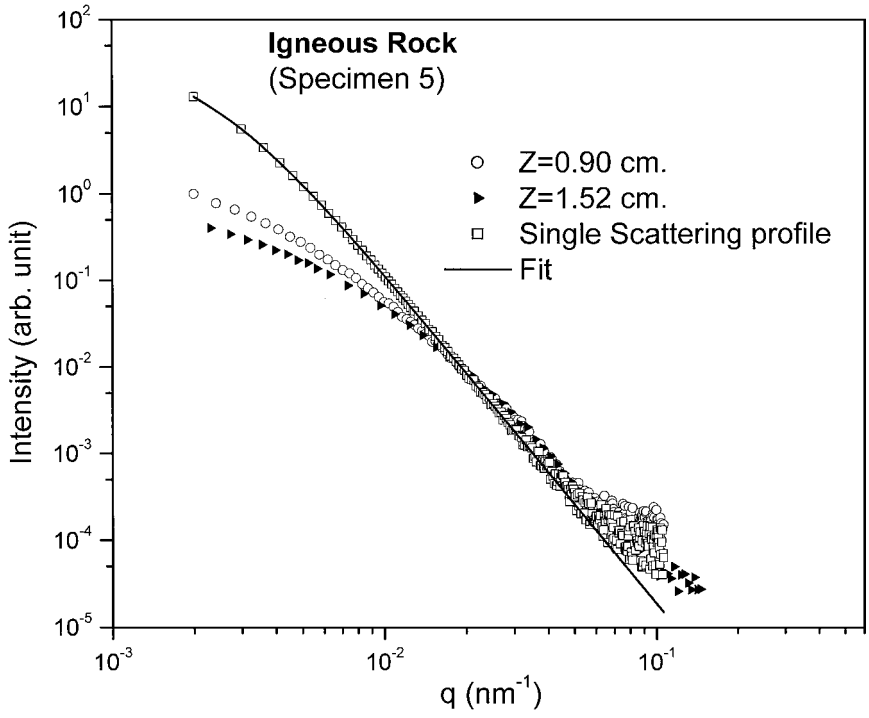

Figure 3 Corrected SANS profiles from specimen-5 (igneous rock) for two thicknesses. The estimated single scattering profile is also shown along-with the fit.

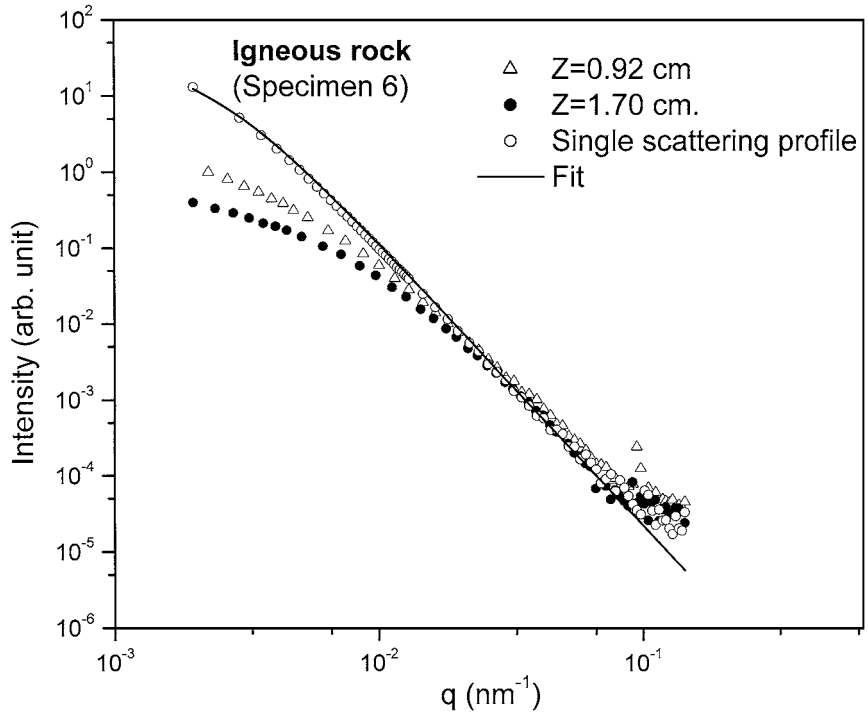

Figure 4 Corrected SANS profiles from specimen-6 (igneous rock) for two thicknesses. The estimated single scattering profile is also shown along-with the fit.

the specimen thickness $Z \leq 0.1L$, where L is the scattering mean free path of the probing radiation in that medium. Multiple scattering [19–22] comes into the picture when the above condition is not valid; i.e. when the specimen thickness is large compared to L and the effect is reflected in the scattering profile by broadening the profile at low q value. A measure of multiple scattering is generally quantified by the scattering power N [22], which is the ratio of sample thickness, Z, to the mean free path, L, of the probing radiation. The single scattering profile can be extracted from the experimentally measured profiles for the two different thicknesses of the specimens [22]. The algorithm for the inversion of multiple scattering profile is based on the principle that although the different multiple scattering profiles are functionally distinct with N, the computed single scattering profiles from each of them are functionally the same or least deviated, provided correct N value is used for the inversion [22]. It is important to note that a region of a SANS profile following a power

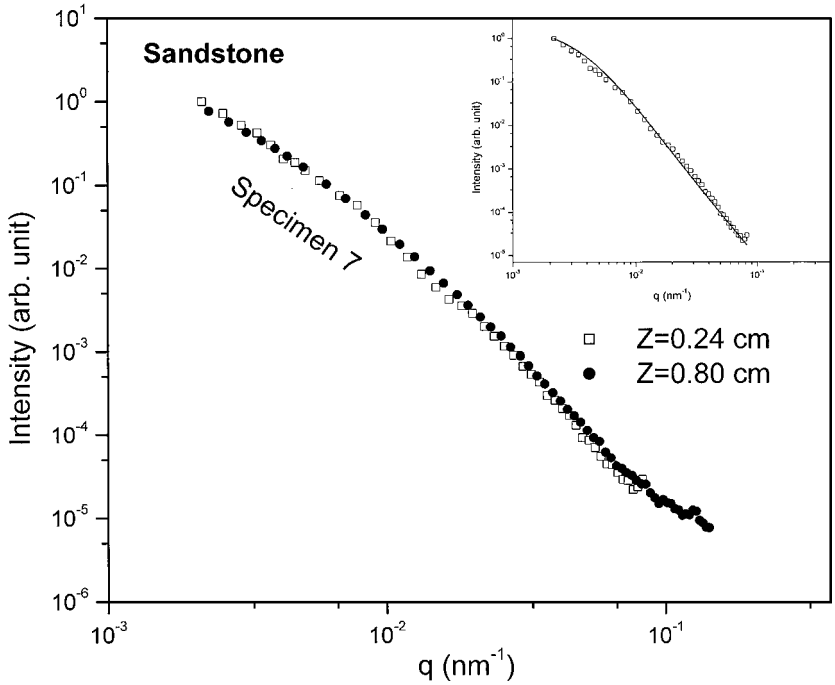

Figure 5 Corrected SANS data from specimen-7 (sandstone from Barakar) for two different thicknesses. Inset shows the fit for the data from 0.24 cm thick specimen.

TABLE I

Specimen no.	Fractal dimension (d_s)	Cut-off length (ξ) (nm.)	Scattering mean free path, L (cm.)
1	2.82 ± 0.11	–	–
2	2.81 ± 0.11	–	–
3	2.84 ± 0.12	–	–
4	2.20 ± 0.13	$\sim$436	0.17 ± 0.04
5	2.37 ± 0.12	$\sim$479	0.25 ± 0.06
6	2.40 ± 0.14	$\sim$427	0.24 ± 0.06
7	2.78 ± 0.16	$\sim$282	–

law, remains unaffected by the effect of multiple scattering [19]. Hence for a fractal object, the profile in the region $q > 1/\xi$ (i.e. in the power law region) should be unaffected by the multiple scattering; however, the region at relatively low q, i.e., for $q \leq 1/\xi$ where power law scattering is not observed due to the upper cut-off of the fractal geometry, is expected to be somewhat affected by multiple scattering.

From the Fig. 1, it is evident that for the specimens 1–3, the profiles follow a power law throughout the accessible q range and the profiles are almost unaffected by the multiple scattering in the above q region. The above profiles have been fitted with the Equation 3 to estimate fractal dimension. Inset of the Fig. 1 shows the fitted curves along with the profiles for the thinner specimens. The estimated fractal dimensions are tabulated in Table I. From Figs 2–4, it is seen that for the specimens 4–6, the effect of multiple scattering is not negligible at relatively lower q value ($q < 10^{-2}$ nm^{-1}) although the regions following the power laws ($q > 10^{-2}$ nm^{-1}) are almost unaffected by multiple scattering. Single scattering profiles for the specimens 4–6 have been estimated and fitted to the Equation 2 using a conventional nonlinear least square method. The single scattering profiles and the fitted curves are shown in Figs 2–4 respectively. The estimated parameters are shown in Table I. For the specimen 7, the functionality of the profiles at two different thicknesses are almost identical and hence without applying any correction for multiple scattering the profile from the thinner specimen has been fitted to the Equation 2 directly. The fit is shown in the inset of Fig 5.

4. Computer simulation

From Table I, it is seen that for the sedimentary (sandstone)/metamorphosed specimens the fractal dimension of the pore grain interface is nearly 2.8. From the SEM micrographs of specimen 7, it is observed that the grains are almost completely covered by fiber like clay/cement. These give rise to highly convoluted surface with high fractal dimension. This relatively high value of the fractal dimension in sedimentary (sandstone)/metamorphosed rocks can be correlated to the formation mechanisms of these rocks. To get an idea about the relation between the formation mechanism of these rocks and the resulting fractal dimension, we present at this stage a computer simulation following the method by Aharonov and Rothman [5]. The simulation starts with a 2 dimensional square lattice that is filled by steps in a checker board manner; i.e., a locally flat interface has a height configuration of $h(x_i) = c_0$ for i even, $h(x_i) = c_0 + 1$ for i odd, where c_0 is a constant. As formation of the sedimentary rocks are associated with deposition and dissolution of small grains, we assign two events, deposition and dissolution, with probability P_+ and P_- respectively. A deposition event corresponds to filling up a randomly chosen site from all the sites those are local minima by a block of height 2. Similarly a dissolution event is defined to be the subtraction of a block of length 2 from a site randomly chosen among all the sites those are local maxima. At each time step a deposition event will occur with a probability $P_+ (1 \geq P_+ \geq 0)$ and a dissolution event will occur with probability P_-. By allowing

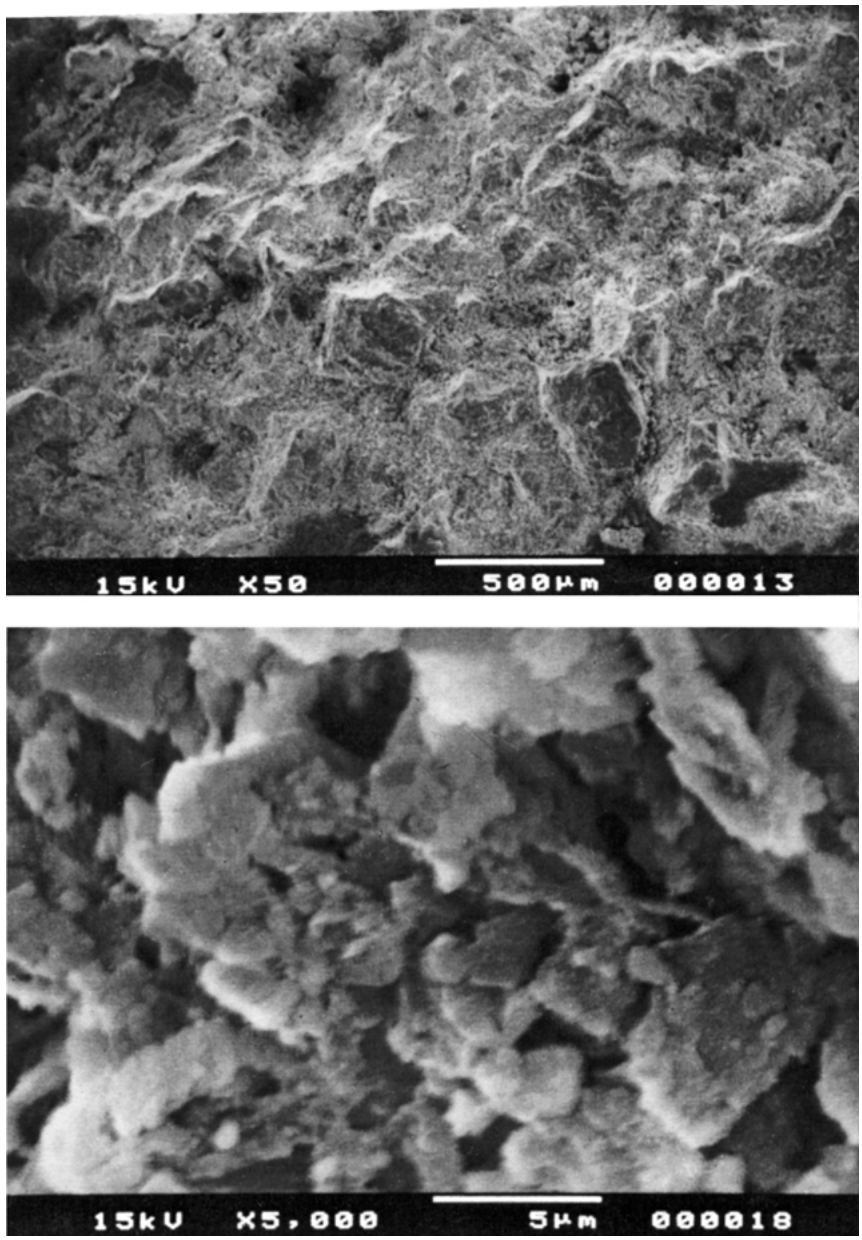

Figure 6 SEM micrographs of the sandstone specimen at two different magnifications.

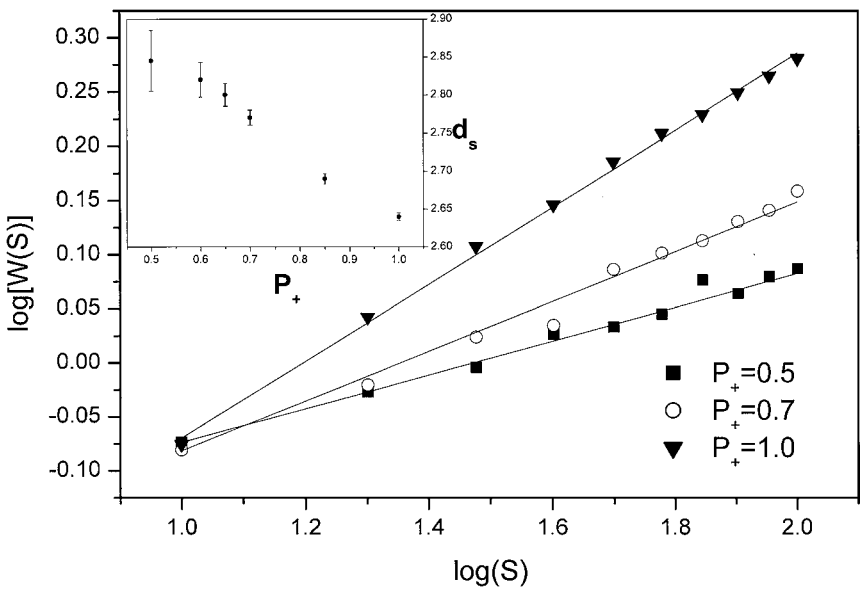

Figure 7 Variation of interface width $W(S)$ with system size for different deposition probability P_+. Solid lines show the fit to a straight line. The inset shows the variation of the surface fractal dimension with P_+.

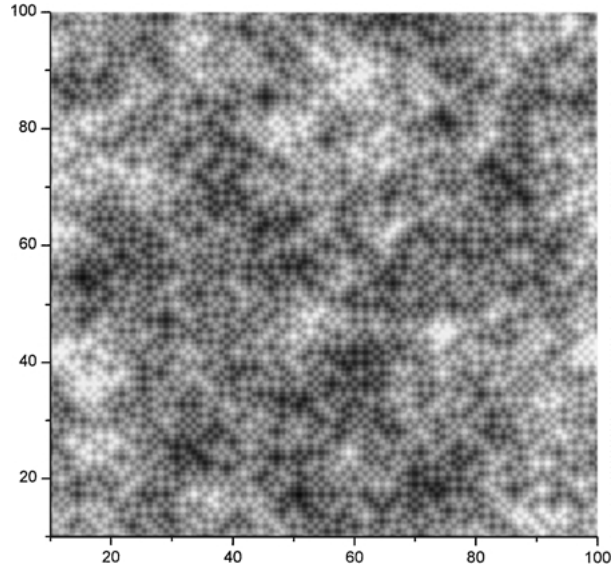

Figure 8 A possible fractal surface taken out of ensemble for fractal dimension ∼2.80 calculated from the computer simulation mentioned in the text based on the formation mechanism of the sedimentary rocks. Darker shadings indicate lower height and lighter shadings indicate higher height.

particles to attach and detach to the interface, effectively we try to simulate molecular exchange across the phase boundaries. To test whether the resulting interfaces are self-affine, the ensemble averaged and saturated interface width $W(S)(=\langle|h(x)-h_{\rm av}|^2\rangle^{1/2})$ ($h_{\rm av}$ is the mean interface height and the angle bracket denote an ensemble average) is measured for different system sizes S. For a fractal surface $W(S)$ should follow a power law in S. The $\log[W(S)]$ vs. $\log(S)$ is plotted and is shown in Fig. 7 for different P_+ values. It is seen that an increase in P_- gives rise to an increase in the surface fractal dimension. Fig. 8. shows an interface taken out of the ensemble for a fractal dimension ∼2.8 for which the simulation has been performed on lattice size 100×100.

5. Conclusion

Pore morphology and the pore surface roughening in some metamorphosed sedimentary rocks, sandstones and igneous rocks have been investigated using SANS which has unfurled the fractal nature of the pore-grain interfaces of these rocks. The metamorphosed rocks and the sandstones possess a surface fractal dimension ∼2.8, while for the igneous rocks the same has been estimated to be ∼2.3. The relatively high value of the fractal dimension in the former case can be attributed to their formation mechanism by molecular exchange across the phase boundaries as examined through a computer simulation model. The multiple scattering effect in these rocks has been investigated from the SANS profiles measured at two different thicknesses of each specimens. For the metamorphosed rocks, the SANS profiles follow a power law over almost the entire accessible q range and hence no unambiguous value of the upper cut-off of the fractal behaviour could be obtained. However, the functionalities of the profiles are not changed appreciably by the effect of multiple scattering. For igneous rocks, a deviation from the power law behaviour due to the upper cut-off of the fractal nature has been observed at a very small q value and the profiles are somewhat affected by multiple scattering in this region. The cut-off value of the fractal geometry and the surface fractal dimension has been estimated from the extracted single scattering profile after correcting for multiple scattering.

Acknowledgements

We are grateful to Dr. S. K. Sikka, Atomic and Condensed Matter Physics Group, B.A.R.C for his encouragement in this work. We thank Drs. K. P. N. Murthy, Materials Science Division, I.G.C.A.R and S. K. Ghosh, Chemistry Division, B.A.R.C for stimulating discussions. We are also grateful to Prof. S. Mitra, Jadavpur University (J.U) for providing the sandstone specimens and Dr. R. Bhar, USIC, J.U for preparing the SEM micrographs.

References

1. A. P. RADLINSKI, E. Z. RADLINSKA, M. AGAMALIAN, G. D. WIGNALL, P. LINDER and O. G. RANDL, *Phys. Rev. Lett.* **82** (1999) 3078.
2. F. TRIOLO, A. TRIOLO, M. M. AGAMILAN, J. S. LIN, R. K. HEENAN, G. LUCIDO and R. TRIOLO, *J. Appl. Cryst.* **33** (2000) 863.
3. P. Z. WONG and J. HOWARD, *Phys. Rev. Lett.* **57** (1986) 637.
4. G. LUCIDO, R. TRIOLO and E. CAPONETTI, *Phys. Rev.* **38** (1988) 9031.
5. E. AHARONOV and D. ROTHMAN, *J. Geophys. Res.* **101** (1996) 2973.
6. S. ROY and S. TARAFDAR, *Phys. Rev.* B **55** (1997) 8038.
7. A. J. KATZ and A. H. THOMPSON, *Phys. Rev. Lett.* **54** (1985) 1325.
8. D. AVNIR, D. FARIN and P. PFEIFER, *Nature* (London) **308** (1984) 261.
9. A. BUNDE and S. HAVLIN (eds.), "Fractals in Science" (Springer Verlag, New York, 1994).
10. M. H. COHEN and M. P. ANDERSON, in "The Chemistry and Physics of Composite Media," edited by M. Tomkiewicz and P. N. Sen (The Electrochemical Society, Pennington, NJ, 1985).
11. S. MAHMOOD NAQVI and J. J. W. ROGERS, "Precambrian Geology of India," Oxford Monograph on Geology and Geophysics No. 6 (Oxford University Press, New York, 1987).
12. D. SEN, S. MAZUMDER, P. SENGUPTA, A. K. GHOSH and V. RAMACHANDHRAN, *J. Macromol. Sci.-Phys.* B **39**(2) (2000) 235.
13. S. MAZUMDER, D. SEN, P. U. M. SASTRY, R. CHITRA, A. SEQUEIRA and K. S. CHANDRASEKARAN, *J. Phys.: Condens Matter* **10** (1998) 9969.
14. D. SEN, S. MAZUMDER, A. SEQUEIRA, A. K. GHOSH and V. RAMACHANDHRAN, M. S. HANRA and B. M. MISRA, *J. Macromol. Sci.-Phys.* B **38**(4) (1999) 341.
15. S. MAZUMDER, D. SEN, T. SARAVANAN and P. R. VIJAYRAGHAVAN, *J. Neutron Research* **9** (2001) 39.
16. P. W. SCHMIDT and R. HEIGHT, *Acta Crystallogr.* **13** (1960) 480.
17. H. D. BALE and P. W. SCHIMIDT, *Phys. Rev. Lett.* **53** (1984) 596.
18. D. SEN, S. MAZUMDER, R. CHITRA and K. S. CHANDRASEKARAN, *J. Mater. Sci.* **36** (2001) 909.
19. S. MAZUMDER and A. SEQUEIRA, *Pramana-J. Phys.* **38** (1992) 95.
20. *Idem.*, *Phys. Rev.* B **39** (1989) 6370.
21. *Idem.*, *ibid.* **41** (1990) 6272.
22. S. MAZUMDER, B. JAYASWAL and A. SEQUEIRA, *Physica* B **241–243** (1998) 1222.

Received 12 March
and accepted 22 October 2001